Characterization of metabolic profiles and lipopolysaccharide effects on porcine vascular wall mesenchymal stem cells

Salvatore Nesci, Chiara Bernardini, Roberta Salaroli, Augusta Zannoni, Fabiana Trombetti, Vittoria Ventrella, Alessandra Pagliarani*, Monica Forni

Department of Veterinary Medical Sciences - University of Bologna

Via Tolara di Sopra, 50 - 40064 Ozzano Emilia (BO), Italy

*Corresponding author: alessandra.pagliarani@unibo.it

Running title: pVW-MSCs metabolic features

Abstract

The link between metabolic remodelling and stem cell fate is still unclear. To explore this topic, the metabolic profile of Porcine Vascular Wall Mesenchymal Stem Cells (pVW-MSCs) was investigated. At the 1st and 2nd cell passages, pVW-MSCs exploit both glycolysis and cellular respiration to synthesize ATP, but in the subsequent (3rd to 8th) passages they don't show any mitochondrial ATP turnover. Interestingly, when the 1st passage pVW-MSCs are exposed to 0.1 or 10 μg/mL lipopolysaccharides (LPS) for 4h, even if ATP synthesis is prevented, the spare respiratory capacity is retained and the glycolytic capacity is unaffected. In contrast, the exposure of pVW-MSCs at the 5th passage to 10 μg/mL LPS stimulates mitochondrial ATP synthesis. Flow cytometry rules out any ROS involvement in the LPS effects, thus suggesting that the pVW-MSC metabolic pattern is modulated by culture conditions via ROS-independent mechanisms.

Keywords: metabolic profiles; cellular acidification; lipopolysaccharide; porcine vascular wall mesenchymal stem cells.

1. INTRODUCTION

The Vascular Wall Mesenchymal Stem Cells are multipotent cells resident in vessels which show an intrinsic pro-angiogenic attitude to differentiate towards endothelial phenotype and to sustain the formation of a capillary network (Psaltis & Simari, 2015). Increasing evidence indicates that vascular stem cells play a fundamental role in angiogenesis and vascular regeneration after damage (Lu & Li, 2018).

Plasticity and adaptation, as well as a broad differentiation capacity, are relevant features of stem cells (L. Zhang et al., 2014). In order to preserve both stem cell potency and self-renewal capability, the maintenance of cellular homeostasis is a critical requirement. Metabolism gathers finely tuned biochemical pathways to match catabolic to anabolic events. Catabolic processes consist of breaking down/oxidation of nutrient-derived compounds (metabolites) to yield energy, while anabolism exploits energy to build macromolecules from simpler precursors. Noteworthy, the rapid stem cell proliferative potential is sustained by anabolic reactions, which synthesize macromolecules and biostructures. Conversely, differentiating cells enhance catabolism to fulfil the bioenergetic demand. Therefore, metabolic adaptations must obey to the specific requirements of diversified functions referable to cell status. A high metabolic flexibility is essential to balance anabolic and catabolic processes so as to adequately maintain the required cell features (Clifford D. L. Folmes, Dzeja, Nelson, & Terzic, 2012). The mitochondrial ATP production from oxidative metabolism is apparently ruled by the cell differentiation and mitochondrial status (C.D.L. Folmes, Dzeja, Nelson, & Terzic, 2012). Indeed, oxidative phosphorylation (OxPhos) re-oxidizes the NADH and $FADH_2$ coenzymes to preserve Krebs cycle activity and to provide the intermediates for fatty acids biosynthesis and *de novo* synthesis of aminoacids and nucleotides (Chandel, Jasper, Ho, & Passegué, 2016). Therefore, mitochondria play an essential role in homeostasis (Lees, Gardner, & Harvey, 2017).

An important question in stem cell metabolism is to identify the energy source, which sustains and addresses cell fate. The main nutrients utilized by stem cells are glucose and glutamine which are oxidized to produce ATP (Tohyama et al., 2016). Most likely, both glutaminolysis, which ensures the reduced coenzymes to fuel OxPhos and the intermediates for the synthesis of macromolecules and biostructures, and glycolysis, support anabolism for cell proliferation (Nesci, 2017). In general, stem cells prefer glycolysis to mitochondrial respiration, but the data on mesenchymal stem cell metabolism are still controversial (Shum, White, Mills, Bentley, & Eliseev, 2016). Probably, proliferation and self-renewal capability are fuelled by glycolysis-dependent anabolic pathways (J. Zhang, Nuebel, Daley, Koehler, & Teitell, 2012). Alternatively, the stemness features, irrespective of proliferative features, may be maintained by the low free radical production under conditions of poor mitochondrial oxidation. However, mitochondrial activity could also be independent of glycolytic regulation (Lisowski, Kannan, Mlody, & Prigione, 2018). Interestingly, during differentiation mesenchymal stem cells (MSCs) from bone marrow maintained glycolytic levels similar to undifferentiated cells (Shum et al., 2016). In addition, when MSCs use glycolysis to sustain metabolism (Chen, Shih, Kuo, Lee, & Wei, 2008), they exhibit a tubular mitochondrial network and a low ROS production (Forni, Peloggia, Trudeau, Shirihai, & Kowaltowski, 2016). The changes in cellular metabolism do not merely result from cell differentiation, but can also be required to allow survival under stress conditions. From this standpoint, the metabolic plasticity would also represent an adaptive strategy to cope with changing conditions. Porcine Vascular Wall Mesenchimal Stem Cells (pVW-MSCs) from the aorta of post-natal pig were isolated, due to the known relevance of swine as excellent model for translational studies (A. Zaniboni et al., 2014).

The present work explores the two major cell metabolic pathways, namely glycolysis and mitochondrial respiration, in pVW-MSCs at different cell passages and under stress conditions induced by lipopolysaccharide (LPS). LPS, naturally produced as component of cell wall by Gram-

negative bacteria, is known to exert profound effects on different stem cell types (Kukolj et al., 2018; Xing, Zhang, Jia, & Xu, 2019; Yin, Zhu, Wang, & Zhao, 2017). Being the role of metabolic changes and mitochondrial function and dynamics in stem cell differentiation still poorly understood (Shum et al., 2016), these studies represent an attempt to cast light on a promising topic, which opens the way to metabolic manipulations to address cell fate.

2. METHODS

2.1. Chemicals

Oligomycin mixture (A:B:C 64:15:17 %), carbonyl cyanide 4-(trifluoromethoxy)phenylhydrazone (FCCP), antimycin A, rotenone, 2-deoxy-glucose (2-DG) were obtained from Vinci-Biochem (Vinci, Italy). 100X antibiotic–antimycotic solution (10,000 units/mL penicillin, 10,000 µg/mL streptomycin, 25 µg/mL Amphotericin B), Dulbecco's Modified Eagle's Medium (DMEM), M199, Fetal Bovine Serum (FBS) and CellROX® Deep Red Flow Cytometry Assay Kit were purchased from Life Technologies (Carlsbad, CA, USA). Trypsin–EDTA solution 1X, lipopolysaccharide (LPS) (*E. coli* 055:B5), and 0,4% Trypan Blue solution were purchased from Sigma-Aldrich (St. Louis, MO, USA). Pericyte Growth Medium (PGM) was purchased from Promocell (Heidelberg, Germany).

2.2. Cell isolation and culture

pVW-MSCs were isolated and characterized from pig thoracic aorta as previously described (A. Zaniboni et al., 2014, 2015). The isolation method consists of two subsequent steps of chemical and physical selection. Briefly, cells were isolated from the media layers through enzymatic digestion and cultured overnight in DMEM 10% FBS plus 10X antibiotic-antimycotic solution in a 5% CO_2 incubator at 38.5°C. The day after, the culture medium was replaced by DMEM plus 10%FBS plus 1X antibiotic-antimycotic solution. Three days after, cells were serum starved overnight and then cultured in DMEM:M199 (1:1), 10% FBS, 1X antibiotic-antimycotic solution. Then cells were trypsinized, grown and expanded in PGM supplemented with 1X antibiotic-antimycotic solution and maintained at 38°C.

2.3. Lipopolysaccharide treatments

Before any treatment, cells were detached by trypsinization, counted in a Burker chamber and stained with 0.4% Trypan Blue to check viability. Aliquots of 6 x 10^5 /mL alive cells (98±2% viability) in PGM were seeded in micro-centrifuge tubes (1 mL) and maintained in incubator under Peltier thermostatation at 38.5 °C and continuous stirring for 4 hours in the presence of the LPS doses to be tested (0, 0.1, 10 µg/mL LPS). The required LPS doses to attain the final concentrations were directly added to the medium.

2.4. Mitochondrial respiration

The oxygen consumption rate (OCR, nmol O_2/min) ascribed to cell respiration was polarographically evaluated by Clark-type electrode using the Oxytherm System (Hansatech Instruments).

OCR values were recorded after sequential addition of inhibitors to evaluate the different conditions under study. The ATP synthase inhibitor oligomycin was used to prevent mitochondrial ATP production and address cells to glycolysis. The ionophore FCCP was employed to uncouple mitochondria. Inhibition of the respiratory chain was obtained by the antimycin A plus rotenone mixture. Basal respiration was detected as baseline OCR before oligomycin addition. Minimal OCR was measured in the presence of 4 μg/mL oligomycin, while maximal respiration was measured after addition of 0.5 μM FCCP. Non-mitochondrial respiration was evaluated in the presence of 1 μg/mL antimycin A plus 4 μM rotenone. The ATP turnover or oligomycin-sensitive respiration was obtained from the decrease in basal respiration after oligomycin addition. The difference between the maximal respiration and the basal respiration provided the spare capacity, which represents the ability to respond to an increased energy demand (Brand & Nicholls, 2011).

2.5. Cellular acidification

The glycolytic function was assayed by the colorimetric detection of L-lactate (Cayman's Glycolysis Cell-Based Assay Kit). This colorimetric assay, widely used for the determination of glycolytic efficiency, evaluates L-lactate, produced by the fermentation of pyruvate, the end product of glycolysis. The lactate dehydrogenase reaction produces NADH, which in turn yields a formazan dye, which absorbs at 490 nm. The formazan amount is proportional to that of L-lactate produced by pVW-MSCs. In each sample the L-lactate concentration was interpolated from the calibration straight line obtained by the detection of fresh L-lactate standards. By this method, the maximal glycolytic capacity was measured in the presence of 4 μg/mL oligomycin, while the non-glycolytic acidification was detected in the presence of 15 mM 2-DG, a glucose analogue which cannot undergo glycolysis and blocks the glycolytic pathway. The glycolytic reserve was obtained as the difference between the L-lactate produced in the presence and in the absence of 4 μg/mL oligomycin.

2.6. Oxidative Stress Evaluation by Flow Cytometry

In order to evaluate if LPS treatment is associated with oxidative stress in pVW-MSCs, CellROX® Deep Red Flow Cytometry Assay Kit was used following manufacturer's instructions. The cell-permeable CellROX® Deep Red reagent is essentially a non-fluorescent compound in the reduced state, but it exhibits a strong fluorogenic signal upon oxidation, thus providing a reliable measure of reactive oxygen species (ROS) in live cells. Blue-fluorescent, cell-impermeant SYTOX ® Blue Dead Cell stain was used to discriminate alive from dead cells. Briefly, pVW-MSCs at 5th passage, were detached by trypsinization and aliquots of 2 x 10^5 cells/mL were treated with 0 μg/mL (Control, C) or 10 μg/mL LPS (treated cells). As a positive control, cells were treated for 60 minutes with the common ROS inducer tert-butyl hydroperoxidase (TBHP). Stained samples were analyzed on MACSQuant Analyzer 10 (Miltenyi Biotec, Bergisch Gladbach, Germany) equipped with 638-nm lasers and 405-nm for the excitation of CellROX®Deep Red and SYTOX® Blue fluorescence, respectively. Fluorescence emission was collected using a 750LP filter and a 450/50BP for CellROX® and SYTOX® Blue, respectively. Data analysis from three independent experiments (n=3) was performed by Flowlogic Software (Miltenyi Biotec, Bergisch Gladbach, Germany).

2.7. Statistical analysis

Statistical analyses were performed by SIGMASTAT software. One-way variance analysis (ANOVA), followed by Student-Newman-Keuls (SNK) test when *F* values indicated significance ($P \leq 0.05$), was applied. The results are expressed as mean ± SD.

3. RESULTS

The metabolic features of pVW-MSCs shifts from OxPhos to glycolysis and are remodelled through cell passages. Accordingly, in the early passages (1st and 2nd), cell respiration and ATP turnover are detectable and mainly attributed to OxPhos, which consumes 30% and 26% ~~of~~ oxygen for ATP synthesis at 1st and 2nd passages respectively. However, in the subsequent cell passages the metabolic pattern of prevailing cell respiration is not maintained (Fig. 1). At all cell passages pVW-MSCs exhibit the maximal respiration when stimulated by FCCP and the spare capacity attains positive values. This pattern indicates oxygen-sensitive mitochondria, maximally at the 5th passage (Fig. 1). LPS treatment differently affects pVW-MSCs, depending on the cell passage and on the LPS dose (Fig. 2). pVW-MSCs at the 1st passage treated for 4 hours with 0.1 μg/mL and 10 μg/mL LPS show an inhibited respiration. However, the inhibition of respiration is apparently removed by oligomycin. Indeed, OCR values show the typical response profile to FCCP and antimycin plus rotenone. The maximal respiration is decreased by both LPS treatments (Fig. 2A). Conversely, lactate production ascribed to glycolysis is not higher in LPS-treated pVW-MSCs than in control values, as it was expected to compensate the failed ATP production by OxPhos. Consistently, the glycolytic capacity, measured as difference in lactate production before and after oligomycin addition, is unaffected by LPS treatment being similar in all pVW-MSCs. Lactate production is inhibited by 2-DG both in LPS-treated and untreated pVW-MSCs (Fig. 2B). A different pattern is shown by the 5° passage pVW-MSCs, which do not show any ATP production apart from 10 μg/mL LPS treated pVW-MSCs (Fig. 2C). Oligomycin increases proton leak, namely the difference in OCR before and after oligomycin addition, in pVW-MSCs which do not perform any mitochondrial ATP synthesis. Irrespective of LPS treatment, FCCP stimulates cellular respiration, while the combination of the two inhibitors antimycin plus rotenone strongly inhibits the maximal oxygen consumption in all pVW-MSCs (Fig. 2C). Lactate production, which attains considerable levels both in untreated and 0.1 μg/mL LPS-treated pVW-MSCs, drops in the 10 μg/mL LPS-treated pVW-MSCs. Accordingly, in the 10 μg/mL LPS-treated pVW-MSCs at the 5th passage a well detectable and oligomycin-sensitive ATP production (Fig. 2C) is associated with an high glycolytic capacity (lactate production in presence of oligomycin) (Fig. 2D). As in all pVW-MSCs at the 1st passage (Fig. 2B), also at the 5th passage pVW-MSCs under all the conditions tested, L-lactate production is inhibited by 2-DG (Fig. 2D).

Flow Cytometry analysis shows that at the 5th passage the 10 μg/mL LPS treatment for 4 hours is not associated to any significant increase in the production of ROS in pVW-MSCs. Accordingly, 3.92% ± 1.62 LPS-treated cells show CellROX® Deep Red reagent strong fluorescent signal similar to the percentage of 2.06% ± 0.33 in control cells. After ROS induction promoted by TBHP treatment, high percentages of pVW-MSCs undergo oxidative stress, in contrast with the basal level of ROS shown both in control and in 10 μg/mL LPS-treated pVW-MSCs (Fig. 3).

4. DISCUSSION

The elucidation of the mechanisms of metabolic switch at different cell passages can help to understand how the modulation of the mitochondrial function affects stem cell fate (Hopkinson et al., 2017). In spite of the wealth of studies, the mechanisms involved in the metabolic rearrangement

under differentiation, widely observed in a variety of stem cells, are still poorly understood. Differentiation is usually featured by a metabolic shift from glycolysis to mitochondrial respiration and, conversely, reprogramming to "maximal stemness" is associated with a rise in glycolysis. There is a general consensus on the observation that the ratio glycolysis/mitochondrial oxidation affects the cell differentiation status. Undifferentiated cells also contain uncoupled and depolarized mitochondria (L. Zhang et al., 2014) and a basal level of reactive oxygen species (ROS), short-lived oxygen-containing molecules which increase during differentiation, thus consuming oxygen and increasing OCR values (L. Zhang et al., 2014).

The results obtained in the present study clearly show that the metabolic profile and the pVW-MSC responses to LPS treatment depend on the passage. As shown in Fig.1, pVW-MSCs at the 1st and 2nd passages depend on OxPhos to produce ATP, which has a mitochondrial origin. Accordingly, in 1st passage pVW-MSCs the increase in the 2DG-dependent lactate production in the presence of oligomycin (Fig. 2B) results from the activation of mitochondrial oxidative metabolism in the presence of a good glycolytic reserve. In the subsequent passages pVW-MSCs do not rely on mitochondrial respiration. The prominent spare respiratory capacity at the 5th passage (Fig. 1) indicates the pVW-MSC propensity to fulfil the energy requirements for differentiation and maturation and also suggests a low efficiency in metabolic reprogramming (Zhou et al., 2017). Apparently, LPS affects the mesenchymal properties of the undifferentiated pVW-MSCs, which have the ability to differentiate in vascular cells (Zaniboni et al., 2015). The mechanisms involved remain to be defined. LPS could inhibit the ATP synthase in pVW-MSCs at 1st passage in the absence of coupling. Accordingly, mitochondria in undifferentiated cells may be uncoupled even before the application of a chemical uncoupler (L. Zhang et al., 2014). However, since pVW-MSCs in presence of FCCP consume oxygen and are susceptive to the antimycin plus rotenone-mixture, irrespective of the treatment, they clearly exploit mitochondrial respiration (Fig. 2A). Noteworthy, at the 1st passage, glycolysis is apparently unaffected by LPS (Fig. 2B). Conversely, the metabolic profile shown by 10 µg/mL LPS-treated pVW-MSCs at 5th passage is typical of mitochondrial oxidative activation (Fig. 2C). Consistently, a low basal oligomycin-sensitive glycolysis is shown, while the glycolytic capacity, detected in the presence of oligomycin, which blocks the mitochondrial ATP synthesis, is apparently stimulated (Fig. 2C, D). Since any increase in apparent glycolytic capacity has been associated with cellular reprogramming and differentiation (Mookerjee, Nicholls, & Brand, 2016), this metabolic profile suggests that stress conditions induced by high LPS doses could stimulate differentiation. Under these conditions, the electron transport chain complexes, and especially complex I by reverse electron transfer (Robb et al., 2018), may enhance the formation of superoxide anion and other ROS. ROS, physiologically produced in mesenchymal stem cells by mitochondrial and extra-mitochondrial reactions, have a recognized role to address differentiation (Atashi, Modarressi, & Pepper, 2015). ROS generation could also explain the higher basal respiration in 10 µg/mL LPS-treated pVW-MSCs with respect to both control and 0.1 µg/mL LPS-treated pVW-MSCs (Fig. 2C) (Piccoli et al., 2005). Differently from all the other conditions tested, the 5th passage 10 µg/mL LPS-treated pVW-MSCs do not show any increase in OCR with respect to the basal respiration when the respiratory chain is blocked by the antimycin plus rotenone mixture (Fig. 2C). The unexpected slight increase in basal OCR may mirror a time-dependent increase in the rate of extra-mitochondrial oxygen-consuming reactions, including ROS formation (Piccoli et al., 2005). Accordingly, the OCR measured after antimycin plus rotenone mixture addition attains similar values under all the conditions tested and is unrelated to mitochondrial bioenergetics. However, quite unexpectedly, even if LPS is usually considered a powerful ROS inducer in mesenchymal stem cells (Yin et al., 2017), cytofluorimetric assays show that the bioenergetic changes in LPS-treated pVW-MSCs are clearly unrelated to ROS generation. LPS is known to interfere with stem cell signaling at

different levels (Yin et al., 2017) and to address lineage commitment (Kukolj et al., 2018; Xing et al., 2019). Probably, the highest LPS concentration tested, through ROS-independent mechanisms which remain to be defined, shifts pVW-MSC metabolism to cell respiration, even if the glycolytic capacity is maintained, to preserve the bioenergetic efficiency under unfavourable conditions. To sum up, if OxPhos is associated with differentiation and glycolysis with multipotency (L. Zhang et al., 2014), apparently high LPS doses, at least under the conditions adopted in the present study, promote in pVW-MSCs a metabolic rearrangement typical of differentiating cells which is apparently unrelated to ROS generation.

The metabolic modulation driven by LPS in pVW-MSCs may help to understand how local mediators and culture conditions can address cell fate. Moreover, since the pVW-MSC metabolic response to LPS depends on the passage, further studies may be addressed to cast light on the most suitable conditions for metabolic manipulations to be exploited in therapy.

CONFLICT OF INTEREST STATEMENT

All authors declare they have no conflict of interest

ACKNOWLEDGEMENTS

The research was financed by RFO grant and Almaidea senior grant, both from the University of Bologna, Italy.

REFERENCES

Atashi, F., Modarressi, A., & Pepper, M. S. (2015). The role of reactive oxygen species in mesenchymal stem cell adipogenic and osteogenic differentiation: a review. *Stem Cells and Development*, *24*(10), 1150–1163. https://doi.org/10.1089/scd.2014.0484

Brand, M. D., & Nicholls, D. G. (2011). Assessing mitochondrial dysfunction in cells. *The Biochemical Journal*, *435*(2), 297–312. https://doi.org/10.1042/BJ20110162

Chandel, N. S., Jasper, H., Ho, T. T., & Passegué, E. (2016). Metabolic regulation of stem cell function in tissue homeostasis and organismal ageing. *Nature Cell Biology*, *18*(8), 823–832. https://doi.org/10.1038/ncb3385

Chen, C.-T., Shih, Y.-R. V., Kuo, T. K., Lee, O. K., & Wei, Y.-H. (2008). Coordinated changes of mitochondrial biogenesis and antioxidant enzymes during osteogenic differentiation of human mesenchymal stem cells. *Stem Cells (Dayton, Ohio)*, *26*(4), 960–968. https://doi.org/10.1634/stemcells.2007-0509

Folmes, C.D.L., Dzeja, P. P., Nelson, T. J., & Terzic, A. (2012). Mitochondria in control of cell fate. *Circulation Research*, *110*(4), 526–529. https://doi.org/10.1161/RES.0b013e31824ae5c1

Folmes, Clifford D. L., Dzeja, P. P., Nelson, T. J., & Terzic, A. (2012). Metabolic plasticity in stem cell homeostasis and differentiation. *Cell Stem Cell*, *11*(5), 596–606. https://doi.org/10.1016/j.stem.2012.10.002

Forni, M. F., Peloggia, J., Trudeau, K., Shirihai, O., & Kowaltowski, A. J. (2016). Murine Mesenchymal Stem Cell Commitment to Differentiation Is Regulated by Mitochondrial Dynamics. *Stem Cells (Dayton, Ohio)*, *34*(3), 743–755. https://doi.org/10.1002/stem.2248

Hopkinson, B. M., Desler, C., Kalisz, M., Vestentoft, P. S., Juel Rasmussen, L., & Bisgaard, H. C. (2017). Bioenergetic Changes during Differentiation of Human Embryonic Stem Cells along the Hepatic Lineage. *Oxidative Medicine and Cellular Longevity*, *2017*, 5080128. https://doi.org/10.1155/2017/5080128

Kukolj, T., Trivanović, D., Djordjević, I. O., Mojsilović, S., Krstić, J., Obradović, H., … Bugarski, D. (2018). Lipopolysaccharide can modify differentiation and immunomodulatory potential of periodontal ligament stem cells via ERK1,2 signaling. *Journal of Cellular Physiology*, *233*(1), 447–462. https://doi.org/10.1002/jcp.25904

Lees, J. G., Gardner, D. K., & Harvey, A. J. (2017). Pluripotent Stem Cell Metabolism and Mitochondria: Beyond ATP. *Stem Cells International*, *2017*, 2874283. https://doi.org/10.1155/2017/2874283

Lisowski, P., Kannan, P., Mlody, B., & Prigione, A. (2018). Mitochondria and the dynamic control of stem cell homeostasis. *EMBO Reports*, *19*(5). https://doi.org/10.15252/embr.201745432

Lu, W., & Li, X. (2018). Vascular stem/progenitor cells: functions and signaling pathways. *Cellular and Molecular Life Sciences: CMLS*, *75*(5), 859–869. https://doi.org/10.1007/s00018-017-2662-2

Mookerjee, S. A., Nicholls, D. G., & Brand, M. D. (2016). Determining Maximum Glycolytic Capacity Using Extracellular Flux Measurements. *PloS One*, *11*(3), e0152016. https://doi.org/10.1371/journal.pone.0152016

Nesci, S. (2017). Glucose and glutamine in the mitochondrial oxidative metabolism of stem cells. *Mitochondrion*, *35*, 11–12. https://doi.org/10.1016/j.mito.2017.04.004

Piccoli, C., Ria, R., Scrima, R., Cela, O., D'Aprile, A., Boffoli, D., … Capitanio, N. (2005). Characterization of mitochondrial and extra-mitochondrial oxygen consuming reactions in human hematopoietic stem cells. Novel evidence of the occurrence of NAD(P)H oxidase activity. *The Journal of Biological Chemistry*, *280*(28), 26467–26476. https://doi.org/10.1074/jbc.M500047200

Psaltis, P. J., & Simari, R. D. (2015). Vascular wall progenitor cells in health and disease. *Circulation Research*, *116*(8), 1392–1412. https://doi.org/10.1161/CIRCRESAHA.116.305368

Robb, E. L., Hall, A. R., Prime, T. A., Eaton, S., Szibor, M., Viscomi, C., … Murphy, M. P. (2018). Control of mitochondrial superoxide production by reverse electron transport at complex I. *The Journal of Biological Chemistry*, *293*(25), 9869–9879. https://doi.org/10.1074/jbc.RA118.003647

Shum, L. C., White, N. S., Mills, B. N., Bentley, K. L. de M., & Eliseev, R. A. (2016). Energy Metabolism in Mesenchymal Stem Cells During Osteogenic Differentiation. *Stem Cells and Development*, *25*(2), 114–122. https://doi.org/10.1089/scd.2015.0193

Tohyama, S., Fujita, J., Hishiki, T., Matsuura, T., Hattori, F., Ohno, R., … Fukuda, K. (2016). Glutamine Oxidation Is Indispensable for Survival of Human Pluripotent Stem Cells. *Cell Metabolism*, *23*(4), 663–674. https://doi.org/10.1016/j.cmet.2016.03.001

Xing, Y., Zhang, Y., Jia, L., & Xu, X. (2019). Lipopolysaccharide from Escherichia coli stimulates osteogenic differentiation of human periodontal ligament stem cells through Wnt/β-catenin-

induced TAZ elevation. *Molecular Oral Microbiology*, *34*(1). https://doi.org/10.1111/omi.12249

Yin, K., Zhu, R., Wang, S., & Zhao, R. C. (2017). Low level laser (LLL) attenuate LPS-induced inflammatory responses in mesenchymal stem cells via the suppression of NF-κB signaling pathway in vitro. *PloS One*, *12*(6), e0179175. https://doi.org/10.1371/journal.pone.0179175

Zaniboni, A., Bernardini, C., Alessandri, M., Mangano, C., Zannoni, A., Bianchi, F., … Forni, M. (2014). Cells derived from porcine aorta tunica media show mesenchymal stromal-like cell properties in in vitro culture. *American Journal of Physiology. Cell Physiology*, *306*(4), C322-333. https://doi.org/10.1152/ajpcell.00112.2013

Zaniboni, A., Bernardini, C., Bertocchi, M., Zannoni, A., Bianchi, F., Avallone, G., … Forni, M. (2015). In vitro differentiation of porcine aortic vascular precursor cells to endothelial and vascular smooth muscle cells. *American Journal of Physiology-Cell Physiology*, *309*(5), C320–C331. https://doi.org/10.1152/ajpcell.00049.2015

Zhang, J., Nuebel, E., Daley, G. Q., Koehler, C. M., & Teitell, M. A. (2012). Metabolic regulation in pluripotent stem cells during reprogramming and self-renewal. *Cell Stem Cell*, *11*(5), 589–595. https://doi.org/10.1016/j.stem.2012.10.005

Zhang, L., Marsboom, G., Glick, D., Zhang, Y., Toth, P. T., Jones, N., … Rehman, J. (2014). Bioenergetic shifts during transitions between stem cell states (2013 Grover Conference series). *Pulmonary Circulation*, *4*(3), 387–394. https://doi.org/10.1086/677353

Zhou, Y., Al-Saaidi, R. A., Fernandez-Guerra, P., Freude, K. K., Olsen, R. K. J., Jensen, U. B., … Luo, Y. (2017). Mitochondrial Spare Respiratory Capacity Is Negatively Correlated with Nuclear Reprogramming Efficiency. *Stem Cells and Development*, *26*(3), 166–176. https://doi.org/10.1089/scd.2016.0162

FIGURE CAPTIONS

Figure 1. Bioenergetic profile of pVW-MSCs at different cell passages. The oxygen consumption rate (OCR), expressed as nmol O_2/min/10^6 cells, was evaluated in the presence of oligomycin (to inhibit

the ATP synthase), FCCP (OxPhos uncoupler) and antimycin plus rotenone (respiratory chain inhibitors), as described in Section 2, to determine the key respiratory parameters: *basal respiration ATP turnover*; *maximal respiration*; *spare capacity*. Data are the mean ± SD (vertical bars) from three experiments carried out on different cell preparations.

Figure 2. LPS effects on pVW-MSC metabolism at 1st and 5th passages. Upper panel: mitochondrial respiration evaluated as oxygen consumption rate (OCR) and expressed as nmol O_2/min/10^6 cells in 1st A) and 5th passage cells C), respectively. Lower panel: glycolytic activity evaluated as L-lactate production in 1st B) and 5th passage cells D), respectively. Data expressed as points (A and C plots) and column chart (B and D plots) represent the mean ± S.D (vertical bars) from three experiments carried out on different cell preparations. In B) and D) plots inhibitors were subsequently added: ( ) no inhibitors; ( ) +4 µg/mL oligomycin; ( ) +15 mM 2-DG; in each plot different upper-case letters indicate significantly different values among different LPS treatments under the same inhibiting conditions; different lower-case letters indicate significantly different values within each LPS treatment (0.0 µg/mL, 0.1 µg/mL, 10 µg/mL LPS) ($P \leq 0.05$).

Figure 3. Representative graphs of ROS evaluation by Flow Cytometry in pVW-MSCs at the 5th passage. 0.0 µg/mL LPS (Control, C) for 4 hours (panel A), 10.0 µg/mL LPS for 4 hours (panel B) and 50 mM TBHP for 60 minutes (Positive Control, panel C) before labeling by CellROX® Deep Red Flow Cytometry Assay Kit.

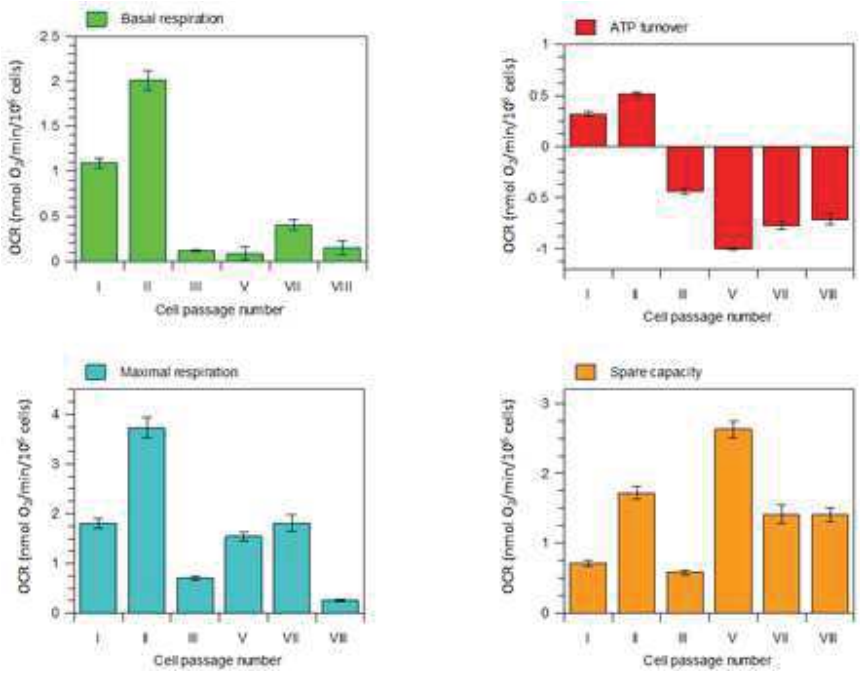

Figure 1. Bioenergetic profile of pVW-MSCs at different cell passages. The oxygen consumption rate (OCR), expressed as nmol O2/min/106 cells, was evaluated in the presence of oligomycin (to inhibit the ATP synthase), FCCP (OxPhos uncoupler) and antimycin plus rotenone (respiratory chain inhibitors), as described in Section 2, to determine the key respiratory parameters: basal respiration ATP turnover; maximal respiration; spare capacity. Data are the mean ± SD (vertical bars) from three experiments carried out on different cell preparations.

37x29mm (300 x 300 DPI)

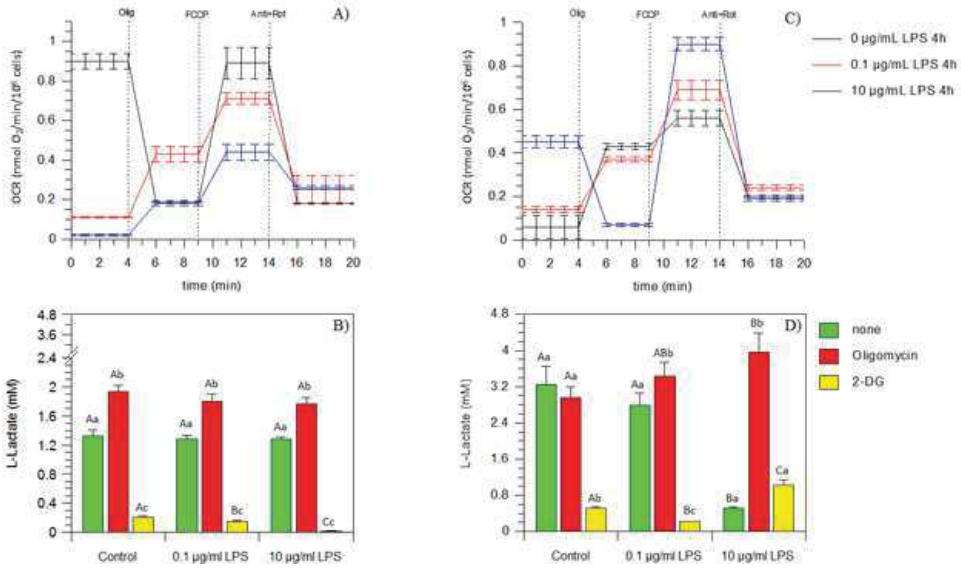

Figure 2. LPS effects on pVW-MSC metabolism at 1st and 5th passages. Upper panel: mitochondrial respiration evaluated as oxygen consumption rate (OCR) and expressed as nmol O2/min/106 cells in 1st A) and 5th passage cells C), respectively. Lower panel: glycolytic activity evaluated as L-lactate production in 1st B) and 5th passage cells D), respectively. Data expressed as points (A and C plots) and column chart (B and D plots) represent the mean ± S.D (vertical bars) from three experiments carried out on different cell preparations. In B) and D) plots inhibitors were subsequently added: (green) no inhibitors; (red) +4 µg/mL oligomycin; (yellow) +15 mM 2-DG; in each plot different upper-case letters indicate significantly different values among different LPS treatments under the same inhibiting conditions; different lower-case letters indicate significantly different values within each LPS treatment (0.0 µg/mL, 0.1 µg/mL, 10 µg/mL LPS) ($P \leq 0.05$).

53x31mm (300 x 300 DPI)

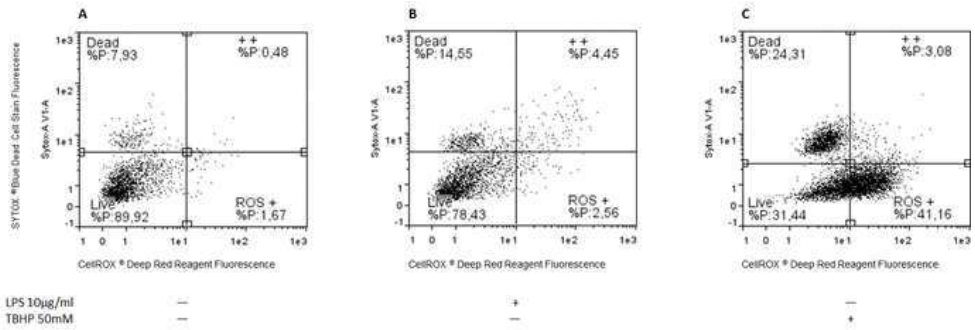

Figure 3. Representative graphs of ROS evaluation by Flow Cytometry in pVW-MSCs at the 5th passage. 0.0 µg/mL LPS (Control, C) for 4 hours (panel A), 10.0 µg/mL LPS for 4 hours (panel B) and 50 mM TBHP for 60 minutes (Positive Control, panel C) before labeling by CellROX® Deep Red Flow Cytometry Assay Kit.

58x19mm (300 x 300 DPI)

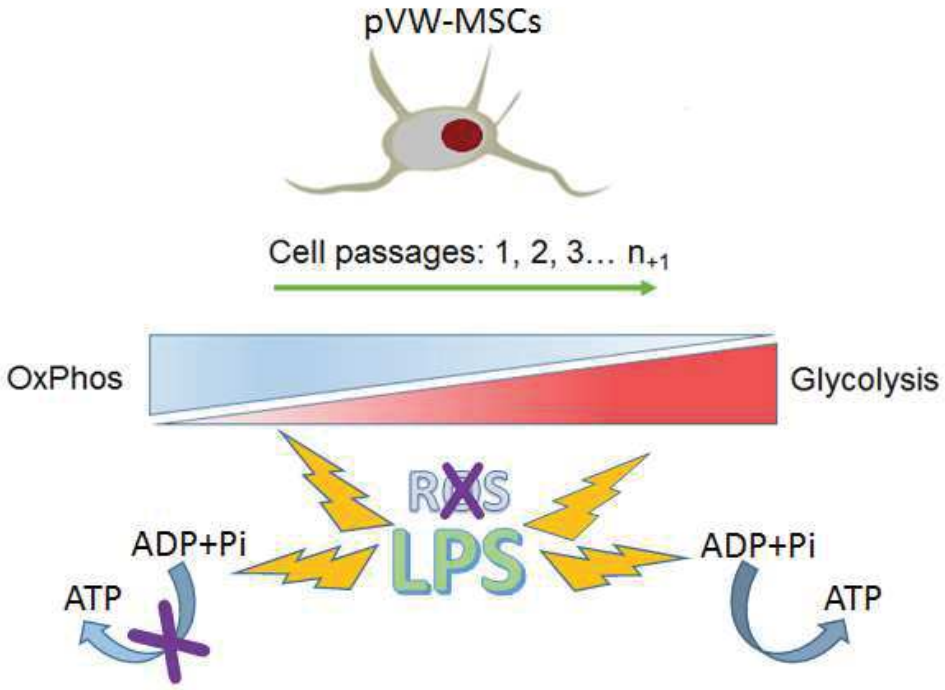

Graphical Abstract

50x40mm (300 x 300 DPI)